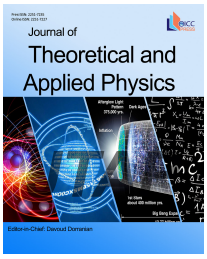

Volume 19, Issue 2, 192525 (1-7)

Journal of Theoretical and Applied Physics (JTAP)

https://doi.org/10.57647/j.jtap.2025.1902.25

Design and analysis of bi-layer graphene based photodetector enhanced by metallic nano-antenna

Mahsa Naghipour[1], Mahdi Zavvari[2,*], Hassan Rasooli Saghai[3]

[1]*Department of Electrical Engineering, Urmia Branch, Islamic Azad University, Urmia, Iran.*
[2]*Antenna and Microwave Research Center, Urmia Branch, Islamic Azad University, Urmia, Iran.*
[3]*Department of Electrical Engineering, Tabriz branch, Islamic Azad University, Tabriz, Iran.*

[*]**Corresponding author:** mahdi.zavvari@iau.ac.ir

Original Research

Received:
5 January 2025
Revised:
10 February 2025
Accepted:
9 April 2025
Published online:
10 April 2025

Abstract:

A new design of graphene-based photodetectors is proposed and studied to be used in near and mid-IR applications. To do so, a bi-layer graphene is implemented as active photo-absorbing region and its absorption spectra was calculated. Based on its response peak, an array of metallic nano rods is designed to be inserted between two layers of graphene and resonate in desired response wavelengths. Such a resonance causes induction and enhancement of incident field in the upper and lower graphene layers and leads to increased absorption. The results show that by using the nano-rods, the mid-IR absorption response of graphene bi-layer is doubled around 6.8 μm, however it is polarization-dependent. We also studied performance characteristics of device such as photo-responsivity, dark and photocurrent and specific detectivity. According the calculations, the proposed photodetector exhibits responsivity as high as about 27 A/W which is higher than previously reported works.

Keywords: Graphene; Photodetector; Plasmonic; Photonic crystals

1. Introduction

By introducing the optical communication as a reliable and more efficient method for data transmission systems, it has earned an uncompetetive and mature state in this field [1–3]. So by development of different components of an optical link, photodetectors have attracted much interest because of their wide applications, not only in the optical communication systems but also in other detection systems such as medical imaging, chemical composition detection, optical sensors, etc [4–8]. In recent years different types of photodetectors have been extensively studied and presented for wide operation areas, whose main difference is in the physics and structure of active absorbing region [9–11]. This variety ranges from simple intrinsic region to quantum nanostructure-based photo-absorbing layers. By introduction of graphene as a material with potential applications in electronics and optics, it's been proposed to be used as the active layer in a photodetector at which it is expected to achieve high performance such as room-temperature operation and consequently different structures have been studied as graphene photodetector at recent decade [12–15].

Recently, several structures based on graphene were demonstrated constructed to study the 1.55 μm light photoresponse properties. Graphene-field effect transistor (FET) was firstly reported with responsivity of 0.5 mA/W [16]. A symmetric metal-graphene-metal photodetector was fabricated and showed a responsivity of 1.5 mA/W [17]. Due to the low absorptivity, zero band gap, lack of gain mechanism and picosecond scale carrier lifetime of graphene, most of Gr-based photodetectors show low responsivity at the level of several to tens of mA/W [17]. It's been shown by Echtermeyer et al. that the efficiency of graphene-based photodetectors can be increased up to 20 times by introducing a plasmonic nanostructures [18]. They showed that by application of metallic nanostructures into the surface of absorbing graphene layer, the optical field concentration is considerably increase which leads to higher absorption efficiency and responsivity. Chang et al. proposed a wide band detector utilizing a two-layer graphene heterostructure with a tunneling barrier. They achieved responsivity higher than 1 A/W with low applied voltage about 1 V. A photo-transistor was proposed in 2018 by Cakmakyapan

et al. based on gold-patched graphene nano-stripes with broadband and ultrafast photodetection with high responsivity. They achieved 0.6 A/W at 0.8 μm and 11.5 A/W at 20 μm responsivity with operation speeds exceeding 50 GHz [19]. M. AlAloul proposed a plasmon-enhanced photothermoelectric graphene detector using CMOS-compatible titanium nitride on the silicon-on-insulator platform. The photodetector responsivity is as high as 1.4 A/W (1.1 A/W external) at an ultra-compact length of 3.5 μm, which is the most compact footprint reported for a graphene-based waveguide photodetector. Furthermore, it operates at zero-bias, consumes zero energy, and has an ultra-low intrinsic noise equivalent power (NEP < 20 pW/Hz$^{0.5}$) [20].

One way to increase the responsivity of a photodetector is to enhance the optical field in absorption region by excitation of localized plasmons. Metallic nanoantennas enhance the optical field primarily through the excitation of localized surface plasmon resonances (LSPRs). LSPRs are collective oscillations of conduction electrons at the interface between a metal and a dielectric, driven by the incident electromagnetic field. These resonances can significantly enhance the local electric field near the surface of the nanoantenna, leading to strong light-matter interactions. When light interacts with a metallic nanoparticle, it can induce a resonant oscillation of the free electrons in the metal. This resonance occurs when the frequency of the incident light matches the natural frequency of the electron cloud oscillation. The resonance condition is given by:

$$\varepsilon_m(\omega) + 2\varepsilon_d = 0 \tag{1}$$

where $\varepsilon_m(\omega)$is the frequency-dependent complex dielectric function of the metal, and $\varepsilon_d$is the dielectric constant of the surrounding medium. At resonance, the induced dipole moment pp in the nanoparticle is greatly enhanced, leading to a strong local electric field E_{loc}:

$$E_{loc} = E_0 + \frac{1}{4\pi\varepsilon_0\varepsilon_d} \cdot \frac{3(p\cdot\acute{r})\acute{r} - p}{r^3} \tag{2}$$

where E_0 is the incident electric field, ε_0 is the permittivity of free space, $\acute{r}$ is the unit vector pointing from the nanoparticle to the observation point, and r is the distance from the nanoparticle.

Recently our team proposed a graphene-based photodetector in which a periodic array of metallic nanostructures placed on the graphene absorbing layer to interact and resonate with the incident beam and hence increase the optical field, leading to enhanced absorption. We studied its two-color detection performance in mid and long IR and responsivities up to 29 A/W was obtained [21]. In this paper we study the effect of an additional graphene layer placed on top of metallic rods on the performance characteristics of detector to extend the response of detector to higher wavelengths in the range of long IR with higher responsivities.

The optical behavior simulation of this structure have been performed using FDTD simulation software and the electrical results of the structure obtained by coding in MATLAB software. It is expected that the combination of top and bottom graphene layers with metallic photonic crystals (MPC) gives a degree of freedom in design of structure for multi-color detection. The rest of the article is as follows: Section 2 describes the characteristics of the proposed structure, section 3 presents the numerical results of the simulation, and section 4 concludes the paper.

2. Device structure and design principles

The proposed photo-detector structure consists of three regions, the p and n regions being designed using Si. While the intrinsic middle layer is designed using graphene, a regular pattern of circular metallic nano-structures as a photonic crystal is placed between two graphene absorbing layers which connects the drain and source. As far as related to operating principle, a signal enters the intrinsic layer of the photo detector. Then some of the signal is reflected there, some is transmitted and the rest is absorbed. The production of an electron-hole pair depends directly on the amount of light absorbed. Since the thickness of graphene is very low, small fraction of the exposed beam is absorbed and in this paper, we exploit two layers of graphene to enhance the amount of absorbed beam. In addition, signal absorption depends on the intrinsic parameters of the proposed structure. Therefore, the goal is to optimize the photo detector structure to receive maximum signal absorption.

Figure 1 shows the schematic of the proposed graphene photodetector containing photonic crystals. The structure consists of a highly doped Si substrate, a SiO_2 dielectric layer, graphene bi-layer as absorption region and charge transfer path and two metallic contacts as drain and source electrodes using Au and Pd on top of each other which are connected through the graphene bi-layer.

As shown in figure 1, a periodic array of metallic rods with finite thickness are placed inside the graphene bi-layer which play the role of a metallic photonic crystal. By using this metallic rods, it is expected to concentrate the incident optical beam into the surface of graphene absorption layers at resonance frequencies and hence increase the absorption and responsivity of detector. In this work we study the effect of using photonic crystal and adding the graphene layer on the performance characteristics of a conventional graphene photodetector. By proper design of this metallic structures to resonate in more frequencies, two or multi-color detection of the photodetector can be achieved. To do so, we use the unit cell of this layer and its equivalent circuit model which are shown in Fig. 2. In the circuit model of a metallic nanorod, the nanorod is typically represented

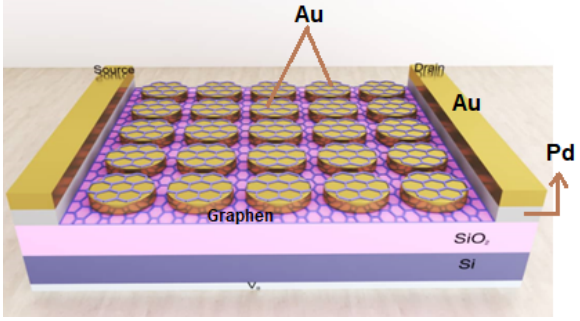

Figure 1. Proposed Graphene bi-layer based photo detector containing photonic crystals.

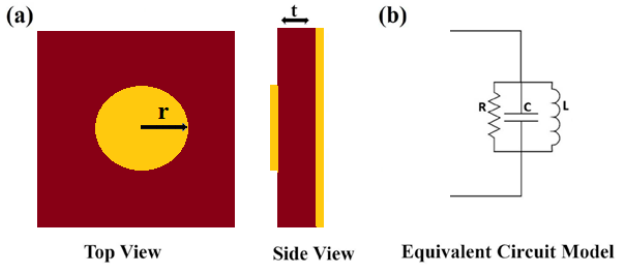

Figure 2. The unit cell of metallic photonic crystal and its equivalent circuit model.

using lumped elements to capture its electromagnetic behavior, particularly in the context of plasmonic resonances and wave propagation.

The model consists of a parallel RLC circuit whose elements are dependent on the geometrical parameters of unit cell. The inductor (L) represents the kinetic energy of the electrons oscillating in the nanorod. The inductance arises due to the inertia of the electron gas in response to an applied electric field. The nanorod's geometry (length, cross-sectional area) and the material's electron density influence the inductance. Longer nanorods or higher electron densities typically result in higher inductance. The resistance accounts for the ohmic losses in the nanorod due to electron scattering and resistive heating. The resistance depends on the material's conductivity, the nanorod's dimensions, and the frequency of operation (due to the skin effect at high frequencies). Losses increase with smaller cross-sectional areas or higher frequencies. Capacitor (C) represents the electrostatic energy stored in the nanorod due to charge accumulation at its ends. The capacitance arises from the polarization of the nanorod when an external electric field is applied. It depends on the nanorod's geometry and the permittivity of the surrounding medium.

The resonant frequency of this circuit can be obtained from [22]:

$$f_r = \frac{1.8412}{2\pi r_e \sqrt{\varepsilon_r}\sqrt{\varepsilon_0 \mu_0}} \tag{3}$$

in which ε_r is relative permittivity of material between conductors, and r_e is effective radius of rods which can be calculated through:

$$r_e = r\left\{1 + \frac{2h}{\pi r \varepsilon_r}\left[\ln\left(\frac{\pi r}{2h}\right) + 1.7726\right]\right\}^{\frac{1}{2}} \tag{4}$$

in which r is radius of rods and h is the spacing of two conductors. Our calculations show that in order to have a resonant frequency with a bi-layer graphene in mid-IR range, rods with 0.1 μm radius should be implemented.

In this work, we used FDTD calculations to obtain the absorption of structure and its response to optical field.

The simulation region includes the arrays ($\Lambda_1 \times \Lambda_2$) and its height is 1 microns. A plane wave light source is located at a distance of 4 micrometers above the structure. In x, y directions, periodic boundary conditions is applied for the structure and the PML boundary condition in the z direction. Fig. 3 illustrates the calculated absorption spectra for the structure with and without photonic crystals. Regarding the

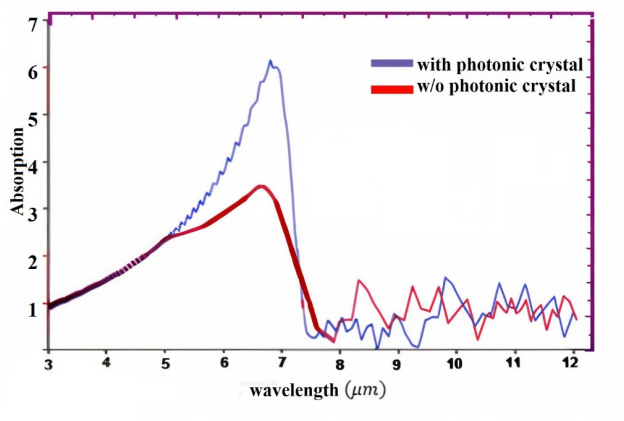

Figure 3. Absorption spectra for the structure with and without photonic crystals.

curves, the absorption is doubled in 6.8 μm wavelength by using the metallic rods and one can be expected that considerable increase in responsivity is achieved. We also studied the absorption response of structure to incident beams with 90° polarization and according to the results depicted in Fig. 4, the absorption peak considerably decreases for that polarization. This challenge is due to the anisotropic nature of nanorods, which typically exhibit strong polarization sensitivity and can be engineered by using some other types of nanostructures such a sphere etc. as the future work.

3. Photodetection performance results and discussion

A main factor to monitor the performance of a photodetector is its responsivity which is defined as the ration of electrical output to optical input power. It measures the capability of device in conversion of optical power to electrical voltage (current). For a photoconductive detector it can be calculated from:

$$R_A = \frac{e}{h\nu}\alpha G \tag{5}$$

in which $h\nu$ is photo energy, α is absorption coefficient in graphene bi-layer and G is photoconductive gain. The

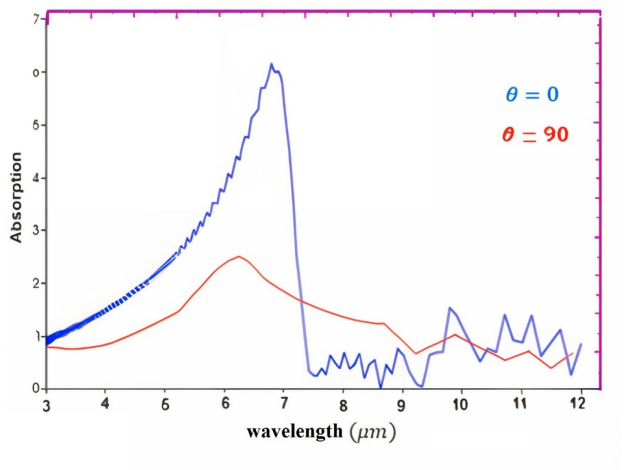

Figure 4. Detector structure response to input light polarization.

photoconductive gain for this structure can be calculated from:

$$G = \frac{2M\tau_R}{\tau_{tr}}\left(1 - e^{-\frac{\tau_{tr}}{\tau_R}}\right) \quad (6)$$

where M is hot carrier factor, τ_{tr} is transit time, and τ_R is recombination lifetime. The transit time can be obtained from:

$$\tau_{tr} = \frac{g}{V_d} \quad (7)$$

where g is the mean distance carrier travel between contacts, and V_d is drift velocity related to carrier mobility. By using the above mentioned relations, the photo-responsivity of proposed device is calculated and results are shown in Fig. 5. According to the figure, a considerable increase about 230% in responsivity of device to mid IR wavelengths (6.8 μm) is achieved by using MPC. We also investigated responsivity in near-IR (0.75 μm) which is arised in the response of graphene bi-layer and amplified by using MPC. It is revealed that the responsivity is also increased for this range of operation but in lower magnitude because it is lies in off-resonance.

The figure also illustrates that for lower applied voltages, the responsivity linearly increases with voltages however for higher values it saturates. The reason can be attributed to the velocity saturation of carriers in higher fields and also contribution of all potential electron-hole pairs in current generation.

Another important characteristic which mainly affects a photodetector operation, is its dark current which degrades device performance by participating as a noisy current. According to the Fig. 6, in lateral cross view of the structure, the possible path for the dark carriers is shown as red arrows which illustrates that these carriers can transit either through graphene or short gold path. So in modeling the equivalent resistance of whole structure, graphene layer resistance (R_G), graphene-metal series resistance (R_S), and contacts resistance (R_C) should be considered. So one can calculate the dark current term of photodetector through the equation

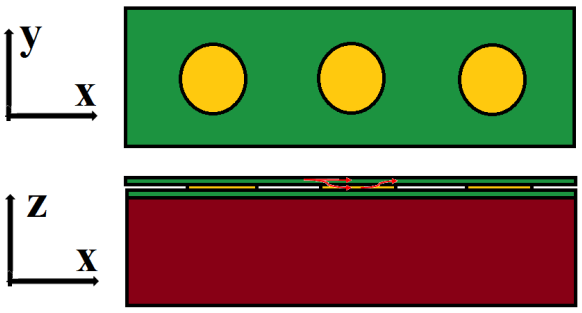

Figure 6. Current flow paths across different regions.

below:

$$I_{ds} = \frac{V_{ds}}{R_G + 2R_C + R_S} \quad (8)$$

Moreover the photocurrent of the photodetector can be obtained from:

$$I_{ph} = e_0 \varphi_{abs} \frac{\tau_i}{\tau_d} \quad (9)$$

$$\tau_i = \left(\frac{1}{\tau_r} + \frac{1}{\tau_d}\right)^{-1} \quad (10)$$

$$\tau_d = \frac{L}{2\mu E} \quad (11)$$

where φ_{abs} is the absorbed light power, τ_i characteristics time, τ_r recombination lifetime, τ_d mean drift time, μ, L and E are carrier mobility, device length and applied field, respectively.

Fig. 7 shows dark and photo-current characteristics of the proposed detector as a function of applied bias and for the cases with and without MPC. A considerable difference in these two current terms is evident according to the figure. However for the structure without MPC, both the currents are in lower level, even its photocurrent is lower than dark current of MPC-based device. This can be attributed to the following reasons: (1) decreased resistance of channel due

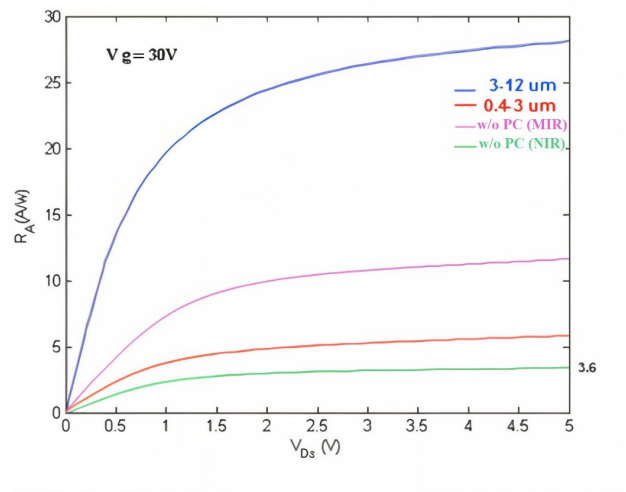

Figure 5. The photo-response of the bi-layer graphene photodetector as a function of the bias voltage (VDS) at VGS = 30 V for two wavelength ranges of 3 – 12 μm and 0.4 – 3 μm with and without photonic crystals.

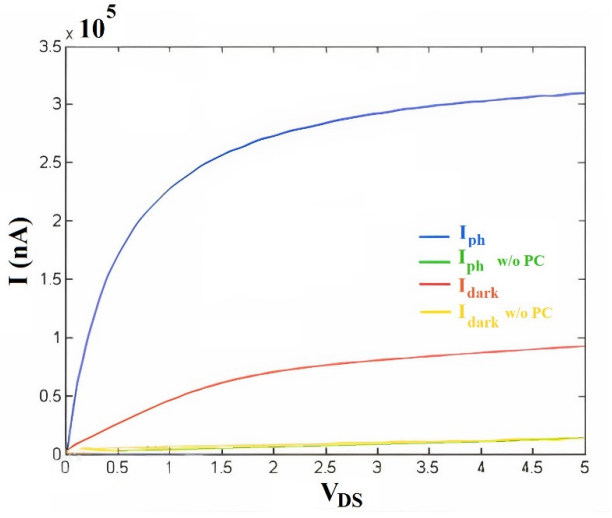

Figure 7. Photo current and dark current of bi-layer graphene photodetector with photonic crystals and without photonic crystals as a function of drain-source voltage at 6.8 micrometers wavelength.

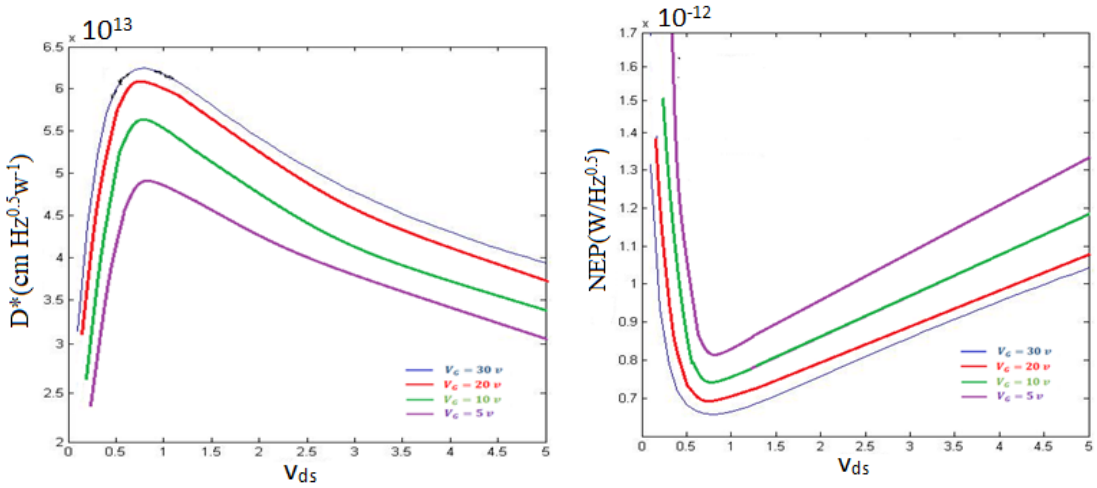

Figure 8. Calculated NEP and specific detectivity (D*) of proposed detector for applied biases and in different gate voltages at 6.8 μm wavelength.

to additional current path from gold rods which reduces total resistance and hence lead to enhanced current flow, (2) lower absorption in Graphene sheet without any additional mechanism to enhance optical field within. That's why the photocurrent is in the order of dark current in this case, and this makes using some.

The currents saturate in higher voltages due to velocity saturation and contribution of all the carriers.

We also calculated NEP and specific detectivity (D^*) of proposed detector for applied biases and in different gate voltages from the equations below:

$$\mathrm{NEP} = \frac{1}{R}\sqrt{2e_0 I_d} \tag{12}$$

$$D^* = \frac{\sqrt{A}}{\mathrm{NEP}} \tag{13}$$

where R is responsivity, I_d is dark current, and A is detector area. The results are shown in Figs. 8. According the figures, the optimum drain-source voltage is around 1 V where the peak detectivity occurs. Moreover for increased gate voltages the efficiency of device is improved. A similar behavior is evident for NEP where indicates the minimum detectable input optical signal and its best point is achieved around 1 V of V_{ds}. Application of higher gate voltage leads to changes in chemical potential of graphene in such a way that more carriers can be incorporated in optical generation and hence in photocurrent generation.

In comparison to previously reported photodetectors at the same wavelength our proposed device shows better response and performance. Table 1 briefly shows the comparison results.

According to the results in Table 1, it can be seen that the proposed detector exhibits much higher responsivity even in room temperature operation. This is an essential requirement for a detector while cooling systems are costly and limit the applications of them. This superior characteristics arise from nanorods presence at the structure. The plasmonic effects of metallic nanorods concentrate electromagnetic fields near their surfaces, leading to a dramatic increase in the interaction between light and graphene. This results in higher photocurrent generation compared to bare graphene or other nanostructured photodetectors. Moreover metallic nanorods facilitate efficient hot carrier injection into graphene. When illuminated, plasmons in the nanorods decay into hot electrons, which are then transferred to the graphene layer. This process is more efficient in nanorod-enhanced systems due to the larger surface area and better coupling between the nanorods and graphene compared to earlier designs using nanoparticles or thin films. Another advantage of nanorods presence is the integration of metallic nanorods with graphene which creates a high electric field at the nanorod-graphene interface, which enhances the separation of photogenerated electron-hole pairs. This leads to a higher photoconductive gain compared to previous designs, where the electric field enhancement was less pronounced. For fabrication of such structure, it should be mentioned

Table 1. Comparison the performance metrics of proposed work with others.

Refs.	Responsivity (A/W)	NEP
[23]	61 (T = 150 K)	NA
[24]	33.8 (T = 50 K)	NA
[25]	0.002	200
[26]	0.014	3
[27]	0.28	2.59×10^{-17}
This work	27.5	7×10^{-13}

that while graphene-based photodetectors enhanced with metallic nanorods offer exciting possibilities for high-speed, broadband, and sensitive photodetection, their fabrication presents significant challenges. Addressing these challenges will require advances in nanofabrication techniques, material quality, and device integration. With continued research and development, these devices could become feasible for practical applications in optoelectronics, telecommunications, and imaging. However, scalability and cost-effectiveness remain key hurdles that must be overcome for widespread adoption.

4. Conclusion

A graphene based photodetector is presented and its performance characteristics was studied. The absorption layer of this device consists of a graphene-bilayer in which the gold nano rods are embedded between two layers of graphene. Our results showed that using such metallic nano antenna lead to field enhancement in graphene absorbing layers and hence the detector responsivity is increased. Our results showed that responsivity as high as 27.5 A/W is achieved in 6.8 μm wavelength which is higher than previously reported detectors in this range of wavelength. Other metrics such as NEP and specific detectivity also show better results in comparison to other previous works.

Authors Contribution
All authors contributed to the study conception and design. Material preparation, data collection and analysis were performed Mahsa Naghipour. The first draft of the manuscript was written by Mahdi Zavvari and all authors commented on previous versions of the manuscript. All authors read and approved the final manuscript.

Availability of data and materials
The data that support the findings of this study are available from the corresponding author, upon reasonable request.

Conflict of interests
The authors declare that they have no known competing financial interests or personal relationships that could have appeared to influence the work reported in this paper.

References

[1] J. Campbell. "Recent advances in telecommunications avalanche photodiodes. ". *IEEE J. Lightwave Technol.*, **25**:109–121, 2007.
DOI: https://doi.org/10.1109/JLT.2006.888481.

[2] I. S. Amiri, A. N. Z. Rashed, H. M. A. Kader, A. A. Al-Awamry, I. A. Abd El-Aziz, P. Yupapin, and G. Palai. "Optical communication transmission systems improvement based on chromatic and polarization Mode dispersion compensation simulation management. ". *Optik*, **207**:163853, 2020.
DOI: https://doi.org/10.1016/j.ijleo.2019.163853.

[3] M. Z. N. Nouri. "Second-harmonic generation in III-nitride quantum wells enhanced by metamaterials.". *IEEE Photon. Technol. Lett.*, **28**: 2199–2202, 2016.
DOI: https://doi.org/10.1109/LPT.2016.2587680.

[4] S. Y. L. Li, J. Qu, F. Zhou, J. Song, and G. Shen. "Recent advances in perovskite photodetectors for image sensing.". *Small*, **17**:2005606, 2021.
DOI: https://doi.org/10.1002/SMLL.202005606.

[5] Q. H. M. Chen, Y. Luo, and X. Tang. "Mid-infrared intraband photodetector via high carrier mobility HgSe colloidal quantum dots. ". *ACS Nano*, **16**:11027–11035, 2022.
DOI: https://doi.org/10.1021/acsnano.2c03631.

[6] M. Zavvari and V. Ahmadi. "Self quenched quantum dot avalanche photodetector for mid-infrared single photon detection.". *Infrared Phys. Technol.*, **62**:7–12, 2014.
DOI: https://doi.org/10.1016/j.infrared.2013.10.005.

[7] A. K. R. S. Bansal, G. Chamundeswari, K. Prakash, P. R. Kumar, A. N. Z. Rashed, M. S. Soliman, and M. T. Islam. "Pt/ZnO and Pt/few-layer graphene/ZnO Schottky devices with Al ohmic contacts using Atlas simulation and machine learning.". *J. Sci. Adv. Mat. Dev.*, **9**, 2024.
DOI: https://doi.org/10.1016/j.jsamd.2024.100798.

[8] A. D. S. Bansal, P. Jain, K. Prakash, K. Sharma, and N. Kumar. "Enhanced optoelectronic properties of bilayer graphene/HgCdTe-based single- and dual-junction photodetectors in long infrared regime.". *IEEE Trans. Nanotech*, **18**:781–789, 2019.
DOI: https://doi.org/10.1109/TNANO.2019.2931814.

[9] L. Y. A. Ren, H. Xu, J. Wu, and Z. Wanga. "Recent progress of III–V quantum dot infrared photodetectors on silicon. ". *J. Mater. Chem. C*, **7**:14441–14453, 2019.
DOI: https://doi.org/10.1039/C9TC05738B.

[10] V. K. A. Yakimov, A. Bloshkin, A. Dvurechenskii, and D. Utkin. "Quantum dot based mid-infrared photodetector enhanced by a hybrid metal-dielectric optical antenna.". *J. Phys. D: Appl. Phys.*, **53**: 335105, 2020.
DOI: https://doi.org/10.1088/1361-6463/ab84a7.

[11] V. K. A. Gupta, S. Bansal, M. H. Alsharif, A. Jahid, and H. S. Cho. "A miniaturized Tri-band implantable antenna for ISM/WMTS/Lower UWB/Wi-Fi frequencies. ". *Sensors*, **23**, 2023.
DOI: https://doi.org/10.3390/s23156989.

[12] T. M. F. H. L. Koppens, Ph. Avouris, A. C. Ferrari, M. S. Vitiello, and M. Polini. "Photodetectors based on graphene, other two-dimensional materials and hybrid systems.". *Nature Nanotech.*, **9**:780–793, 2014.
DOI: https://doi.org/10.1038/nnano.2014.215.

[13] R.-J. S. X. Gan, Y. Gao, I. Meric, T. F. Heinz, K. Shepard, J. Hone, S. Assefa, and D. Englund. "Chip-integrated ultrafast graphene photodetector with high responsivity. ". *Nature Photon.*, **7**:883–887, 2013.
DOI: https://doi.org/10.1038/nphoton.2013.253.

[14] M. Z. H. Faezinia. "Quantum modeling of light absorption in graphene based photo-transistors.". *J. Optoelec. Nanostruct.*, **2**: 9–20, 2017.
DOI: https://doi.org/20.1001.1.24237361.2017.2.1.2.6.

[15] S. Bansal. "Long-wave bilayer graphene/HgCdTe based GBp type-II superlattice unipolar barrier infrared detector.". *Results in Optics*, **12**, 2023.
DOI: https://doi.org/10.1016/j.rio.2023.100425.

[16] T. M. F. Xia, Y.-M. Lin, A. Valdes-Garcia, and P. Avouris. "Ultrafast graphene photodetector.". *Nature Nanotech.*, **4**:839–843, 2009.
DOI: https://doi.org/10.1038/nnano.2009.292.

[17] C. Wang, Y. Dong, Z. Lu, S. Chen, K. Xu, Y. Ma, G. Xu, X. Zhao, and Y. Yu. "High responsivity and high-speed 1.55 μm infrared photodetector from self-powered graphene/Si heterojunction.". *Sensors Act. A*, **291**:87–92, 2019.
DOI: https://doi.org/10.1016/j.sna.2019.03.054.

[18] T. J. Echtermeyer, L. Britnell, P. K. Jasnos, A. Lombardo, R. V. Gorbachev, A. N. Grigorenko, et al. "Strong plasmonic enhancement of photovoltage in graphene.". *Nature Comm.*, **2**:458, 2011.
DOI: https://doi.org/10.1038/ncomms1464.

[19] P. K. L. S. Cakmakyapan, A. Navabi, and M. Jarrahi. "Gold-patched graphene nano-stripes for high-responsivity and ultrafast photodetection from the visible to infrared regime.". *Light Sci. Appl.*, **7**:20, 2018.
DOI: https://doi.org/10.1038/s41377-018-0020-2.

[20] M. R. M. AlAloul. "Plasmon-enhanced graphene photodetector with CMOS-compatible titanium nitride.". *J. Opt. Soc. Am. B*, **38**:602–610, 2021.
DOI: https://doi.org/10.1364/JOSAB.416520.

[21] M. Z. M. Naghipoor and H. Rasooli Saghai. "Two-color photodetection of graphene-based transistors enhanced by metallic photonic crystals. ". *J. Comput. Electron.*, **21**:953–959, 2022.
DOI: https://doi.org/10.1007/s10825-022-01886-w.

[22] K. R. H. S. Choudhary. "Numerical investigation of disordered patch resonator absorbers. ". *App. Phys. A*, **125**:603, 2019.
DOI: https://doi.org/10.1007/s00339-019-2904-2.

[23] S. Fukushima, M. Shimatani, S. Okuda, S. Ogawa, Y. Kanai, T. Ono, K. Inoue, and K. Matsumoto. "Photogating for small high-responsivity graphene middle-wavelength infrared photodetectors. ". *Opt. Eng.*, **59**:037101, 2020.
DOI: https://doi.org/10.1117/1.OE.59.3.037101.

[24] S. Fukushima, M. Shimatani, S. Okuda, S. Ogawa, et al. "High responsivity middle-wavelength infrared graphene photodetectors using photo-gating.". *App. Phys. Lett.*, **113**:061102, 2018.
DOI: https://doi.org/10.1063/1.5039771.

[25] X. Chen, X. Lu, B. Deng, O. Sinai, Y. Shao, C. Li, S. Yuan, V. Tran, K. Watanabe, T. Taniguchi, et al. "Widely tunable black phosphorus mid-infrared photodetector. ". *Nature Comm.*, **8**:1672, 2017.
DOI: https://doi.org/10.1038/s41467-017-01978-3.

[26] M. Long, A. Gao, P. Wang, H. Xia, C. Ott, C. Pan, Y. Fu, E. Liu, X. Chen, W. Lu, T. Nilges, J. Xu, et al. "Room temperature high-detectivity mid-infrared photodetectors based on black arsenic phosphorus.". *Sci. Adv.*, **3**, 2017.
DOI: https://doi.org/10.1126/sciadv.1700589.

[27] K. P. S. Bansal, K. Sharma, N. Sardana, S. Kumar, N. Gupta, and A. K. Singh. "A highly efficient bilayer graphene/ZnO/silicon nanowire based heterojunction photodetector with broadband spectral response.". *Nanotech.*, **31**:202, 2020.
DOI: https://doi.org/10.1088/1361-6528/ab9da8.